2D MULTIZONE SOUND FIELD SYNTHESIS WITH INTERIOR-EXTERIOR AMBISONICS

Takuma Okamoto

National Institute of Information and Communications Technology
3-5, Hikaridai, Seika-cho, Soraku-gun, Kyoto, 619-0289, Japan
okamoto@nict.go.jp

ABSTRACT

This paper presents a two-dimensional multizone sound field synthesis method based on sound field separation and interior-exterior higher-order Ambisonics (HOA) using two circular loudspeaker arrays. In the conventional methods using a circular loudspeaker array, multiple target local sound zones are represented as a global interior sound field. However, the control accuracy of the conventional methods is strongly dependent on the positional relationship between the wavefront direction in a bright zone and other dark zones. This is known as the occlusion problem. On the other hand, the global sound field is defined as a mixture of the interior and exterior sound fields based on sound field separation in the proposed method. The separated global interior and exterior sound fields are then simultaneously synthesized via interior-exterior HOA using two circular loudspeaker arrays with a cylindrical baffle to avoid the forbidden frequency problem in exterior HOA. The results of computer simulations demonstrate that the proposed method using the two circular arrays can successfully avoid the occlusion problem and realize higher control accuracy than the conventional methods using a single circular array.

Index Terms— Multizone sound field synthesis, occlusion problem, interior-exterior sound field separation, interior-exterior sound field synthesis, higher-order Ambisonics

1. INTRODUCTION

Compared with standard sound field synthesis methods, e.g., higher-order Ambisonics (HOA) [1,2], and acoustic contrast control methods [3,4], multizone sound field synthesis can not only synthesize a desired sound field in a bright zone but also maximize the acoustic contrast between the bright zone and the remaining dark zones simultaneously [5]. Both pressure-matching-based [6–12] and mode-matching-based [13–21] methods are investigated.

To synthesize all wavefront directions in a bright zone, a circular loudspeaker array is typically used in both 2D and 2.5D multizone sound field synthesis [6, 7, 9, 13–18, 20, 21]. However, the control accuracy of the conventional methods using a circular array is strongly dependent on the positional relationship between the wavefront direction in a bright zone and the remaining dark zones. This is called the occlusion problem [6, 7, 16].

To alleviate the occlusion problem in multizone sound field synthesis, this paper proposes a two-dimensional multizone sound field synthesis method based on a combination of sound field separation [22, 23] and interior-exterior HOA [24–26] using two circular loudspeaker arrays with a cylindrical baffle, as illustrated in Fig. 1.

This study was partly supported by JSPS KAKENHI under Grant Number JP18K11387.

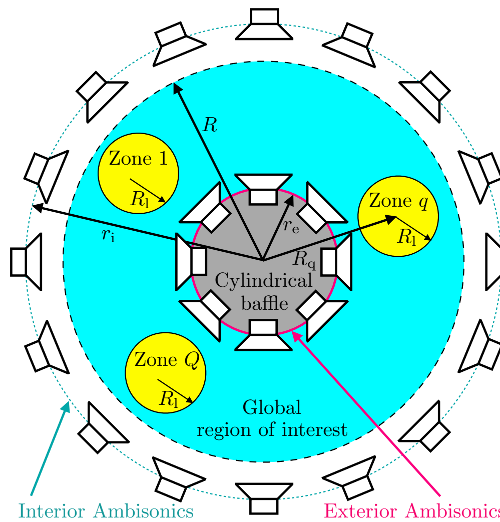

Figure 1: Geometry of proposed multizone sound field control using two circular loudspeaker arrays with a cylindrical baffle.

By introducing exterior sound field decomposition and synthesis, the proposed method is expected to improve the global sound field representation and the control accuracy for multizone sound field synthesis.

In the conventional methods [13, 16, 17, 21], multiple target local sound fields are represented by a global interior sound field for interior mode-matching-based synthesis using a single circular array. However, this representation, which only considers interior sound fields, has limitations in principle and causes the occlusion problem [16]. This problem is also encountered in the pressure-matching-based methods [6,7]. In contrast, the global sound field is defined as a mixture of the interior and exterior sound fields based on sound field separation [22,23] in the proposed method. The separated global interior and exterior sound fields are then simultaneously synthesized through interior-exterior HOA [24–26] using two circular loudspeaker arrays.

Although the proposed method is formulated in a 2D height-invariant sound field using circular loudspeaker arrays based on 2D cylindrical harmonic expansion for simplicity [16,26], the proposed method can also be easily extended to form height-variant 3D sound fields using spherical loudspeaker arrays based on spherical harmonic expansion for real world implementation [19].

To ensure the reproducibility of this study, the MATLAB code used in the simulations conducted in Section 3 is available online.[1]

[1] http://www.okamotocamera.com/waspaa2021.html

© 2021 IEEE. Personal use of this material is permitted. Permission from IEEE must be obtained for all other uses, in any current or future media, including reprinting/republishing this material for advertising or promotional purposes, creating new collective works, for resale or redistribution to servers or lists, or reuse of any copyrighted component of this work in other works.

2. PROPOSED METHOD

2.1. Global interior and exterior sound fields based on sound field separation

Although the multiple target local interior sound fields are represented as a global interior sound field in the conventional methods [13,16,17,21], the global sound field in the proposed method is defined as a mixture of the interior and exterior sound fields based on sound field separation [22,23].

The 2D cylindrical decomposition of a 2D sound field at a point $\boldsymbol{r} = [r, \phi]$ due to a sound source located at $\boldsymbol{r}_\mathrm{s} = [r_\mathrm{s}, \phi_\mathrm{s}]$ is described as [22,27,28]:

$$S_\mathrm{i}(\boldsymbol{r}) = \sum_{m=-\infty}^{\infty} \mathring{A}_m J_m(kr) e^{jm\phi} \qquad \text{for } r_\mathrm{s} > r, \tag{1}$$

$$S_\mathrm{e}(\boldsymbol{r}) = \sum_{m=-\infty}^{\infty} \mathring{B}_m H_m(kr) e^{jm\phi} \qquad \text{for } r_\mathrm{s} < r, \tag{2}$$

where $j = \sqrt{-1}$, k is the wavenumber, $\mathring{A}_m$ and $\mathring{B}_m$ are the 2D cylindrical harmonic spectra of the interior and exterior sound fields, respectively. J_m and H_m are the Bessel function and the Hankel function of the first kind, respectively [27]. The 2D interior-exterior mixed sound field is then defined as [22]:

$$S_\mathrm{i+e}(\boldsymbol{r}) \simeq \sum_{m=-M_\mathrm{i}}^{M_\mathrm{i}} \mathring{A}_m J_m(kr) e^{jm\phi} + \sum_{m=-M_\mathrm{e}}^{M_\mathrm{e}} \mathring{B}_m H_m(kr) e^{jm\phi}, \tag{3}$$

where $M_\mathrm{i} = \lceil ekr/2 \rceil$ and $M_\mathrm{e} = \lceil ekr_\mathrm{s}/2 \rceil$ represent the truncation limits of the 2D cylindrical harmonic orders, and $\lceil \cdot \rceil$ is the ceiling function [29].

When Q local sound zones are assumed and the radius of each zone is R_l (Fig. 1), the truncation limit of the 2D cylindrical harmonic order for the Q local interior sound fields is $M = \lceil ekR_\mathrm{l}/2 \rceil$. Each local interior sound field is centered at $\boldsymbol{r}_q = [R_q, \phi_q]$. Although the 2D cylindrical and 3D spherical harmonic spectra of the local interior sound fields are obtained from sound pressures recorded using 2D and 3D higher-order microphones in sound field analysis and separation [23,28], the 2D cylindrical harmonic spectra for each interior local sound field $\mathring{A}_m^{(q)}$ can be given directly, e.g., as plane and cylindrical waves, in multizone sound field synthesis.

By applying the addition theorem for Bessel and Hankel functions [30] to (3) as 3D sound field separation [23], each local interior sound field $\mathring{A}_m^{(q)}$ can also be represented as:

$$\mathring{A}_m^{(q)} \simeq \sum_{n=-M_\mathrm{i}}^{M_\mathrm{i}} \mathring{A}_n J_{m-n}(kR_q) e^{j(n-m)(\pi+\phi_q)} + \sum_{n=-M_\mathrm{e}}^{M_\mathrm{e}} \mathring{B}_n H_{m-n}(kR_q) e^{j(n-m)(\pi+\phi_q)}. \tag{4}$$

(4) can then be rewritten in matrix form as $\boldsymbol{a} = \boldsymbol{T}\boldsymbol{b}$, where $\boldsymbol{a} = [\mathring{A}_{-M}^{(1)}, \cdots, \mathring{A}_{M}^{(1)}, \cdots, \mathring{A}_{-M}^{(Q)}, \cdots, \mathring{A}_{M}^{(Q)}]^\mathsf{T}$ is a $(2M+1)Q \times 1$ vector for the 2D cylindrical harmonic spectra of the local interior sound fields, $\boldsymbol{T} = [\boldsymbol{T}_\mathrm{i}\ \boldsymbol{T}_\mathrm{e}]$,

$$\boldsymbol{T}_\mathrm{i} = \begin{bmatrix} T_{(-M+M_\mathrm{i})}^{(1)} & \cdots & \cdots & \cdots & T_{(-M-M_\mathrm{i})}^{(1)} \\ \vdots & \vdots & \vdots & \vdots & \vdots \\ T_{(M+M_\mathrm{i})}^{(Q)} & \cdots & \cdots & \cdots & T_{(M-M_\mathrm{i})}^{(Q)} \end{bmatrix}$$

is a $(2M+1)Q \times (2M_\mathrm{i}+1)$ matrix and $T_l^{(q)} = J_l(kR_q)e^{-jl(\pi+\phi_q)}$,

$$\boldsymbol{T}_\mathrm{e} = \begin{bmatrix} T_{(-M+M_\mathrm{e})}^{\prime(1)} & \cdots & \cdots & \cdots & T_{(-M-M_\mathrm{e})}^{\prime(1)} \\ \vdots & \vdots & \vdots & \vdots & \vdots \\ T_{(M+M_\mathrm{e})}^{\prime(Q)} & \cdots & \cdots & \cdots & T_{(M-M_\mathrm{e})}^{\prime(Q)} \end{bmatrix}$$

is a $(2M+1)Q \times (2M_\mathrm{e}+1)$ matrix, $T_l^{\prime(q)} = H_l(kR_q)e^{-jl(\pi+\phi_q)}$, and $\boldsymbol{b} = [\mathring{A}_{-M_\mathrm{i}}, \cdots, \mathring{A}_{M_\mathrm{i}}, \mathring{B}_{-M_\mathrm{e}}, \cdots, \mathring{B}_{M_\mathrm{e}}]^\mathsf{T}$ is a $2(M_\mathrm{i} + M_\mathrm{e} + 1) \times 1$ vector for the 2D cylindrical harmonic spectra of the global interior-exterior mixed sound field. The Q local interior sound fields can then be separated into global interior and exterior sound fields as $\boldsymbol{b} = \boldsymbol{T}^+\boldsymbol{a}$ [23], where $\boldsymbol{T}^+$ is the pseudoinverse of $\boldsymbol{T}$.

In [16], three objective performance measures are defined for multizone sound field synthesis:

1. **Acoustic contrast:** the ratio of the averaged acoustic energy densities of the bright and dark zones;
2. **Bright zone error:** the averaged error between the desired and synthesized sound fields in the bright zone;
3. **Array effort:** a measure proportional to the loudspeaker power consumption required to synthesize the desired multizone sound field.

These objective performance measures can also be applied to the proposed method with the global interior-exterior mixed sound field. An optimal solution for multizone sound field synthesis can then be derived as [16,17]:

$$\boldsymbol{b}_\mathrm{opt} = [\boldsymbol{T}_\mathrm{b}^*\boldsymbol{T}_\mathrm{b} + \lambda_1\boldsymbol{T}_\mathrm{d}^*\boldsymbol{T}_\mathrm{d} + \lambda_2\boldsymbol{I}]^{-1}\boldsymbol{T}_\mathrm{b}^*\boldsymbol{A}_\mathrm{b}, \tag{5}$$

where $\boldsymbol{T}_\mathrm{b}$ and $\boldsymbol{T}_\mathrm{d}$ are the translation matrices for the local bright and dark zones from the global system, respectively, $\boldsymbol{A}_\mathrm{b}$ is the matrix for the 2D cylindrical harmonic spectra for the local bright zones, $(\cdot)^*$ denotes the Hermitian transpose, $\boldsymbol{I}$ is an identity matrix with dimension $2(M_\mathrm{i} + M_\mathrm{e} + 1)$, and λ_1 and λ_2 are the positive Lagrange multipliers. Using (5), the Q local interior sound fields are optimally separated into global interior and exterior sound fields for multizone sound field synthesis via interior-exterior HOA.

2.2. Analytical driving functions for interior-exterior HOA using two circular loudspeaker arrays with a cylindrical baffle

In the proposed method, the separated global interior and exterior sound fields $\boldsymbol{b}_\mathrm{opt}$ derived in (5) are simultaneously synthesized using two circular arrays of omnidirectional loudspeakers with radii of r_i and r_e centered at the origin for interior and exterior HOA [24–26], respectively, as shown in Fig. 1.

Under the free-field assumption, as in the conventional method [13], the driving function for a continuous circular source with radius r_i centered at the origin for the interior 2D HOA is analytically obtained as [1,2]:

$$\mathring{D}_m(r_\mathrm{i}) = -\frac{2j\mathring{A}_m}{\pi H_m(kr_\mathrm{i})}. \tag{6}$$

Although the driving function of a continuous circular source of radius r_e for the exterior HOA is also analytically derived as $-2j\mathring{B}_m/\pi J_m(kr_\mathrm{e})$, this function is sometimes unstable because of the forbidden frequency problem, where $J_m(kr_\mathrm{e}) = 0$ [26,27].

To avoid the forbidden frequency problem for the exterior HOA and thus derive a stable driving function, a cylindrical baffle with radius r_e centered at the origin is introduced [31] and a circular source for the exterior HOA is mounted on the baffle, as shown in Fig. 1. When the cylindrical baffle is introduced, the sound pressure at a point $\boldsymbol{r}$ synthesized using a continuous circular source with radius r_0 centered at the origin is represented by:

$$S(\boldsymbol{r}) = \int_0^{2\pi} D(\boldsymbol{r}_0) G_\mathrm{B}(\boldsymbol{r}, \boldsymbol{r}_0) d\phi_0, \tag{7}$$

where $D(\boldsymbol{r}_0)$ is the driving function for the circular source and $G_\mathrm{B}(\boldsymbol{r}, \boldsymbol{r}_0)$ is the transfer function from the sound source position $\boldsymbol{r}_0 = [r_0, \phi_0]$ to the receiver position $\boldsymbol{r}$. Under the free-field assumption, $G_\mathrm{B}(\boldsymbol{r}, \boldsymbol{r}_0)$ is analyticall given as [27]:

$$G_\mathrm{B}(\boldsymbol{r}_<, \boldsymbol{r}_0) = \sum_{m=-\infty}^{\infty} \frac{j}{4} \Gamma_m(r, r_\mathrm{e}) H_m(kr_0) e^{-jm\phi_0} e^{jm\phi}, \tag{8}$$

$$G_\mathrm{B}(\boldsymbol{r}_>, \boldsymbol{r}_0) = \sum_{m=-\infty}^{\infty} \frac{j}{4} \Gamma_m(r_0, r_\mathrm{e}) H_m(kr) e^{-jm\phi_0} e^{jm\phi}, \tag{9}$$

$$\Gamma_m(r, r_\mathrm{e}) = J_m(kr) - \frac{J'_m(kr_\mathrm{e})}{H'_m(kr_\mathrm{e})} H_m(kr), \tag{10}$$

where J'_m and H'_m are the derivatives of J_m and H_m, respectively.

When the 2D cylindrical harmonic expansion is applied to (7) and (8), the circular convolution theorem then holds, [1, 25, 26, 31] and the sound pressure produced by the interior HOA with $\mathring{D}_m(r_\mathrm{i})$ is represented by:

$$\mathring{S}_m(r_<, r_\mathrm{i}) = \frac{j\pi}{2} \mathring{D}_m(r_\mathrm{i}) \Gamma_m(r, r_\mathrm{e}) H_m(kr_\mathrm{i}) \tag{11}$$

$$= \mathring{A}_m J_m(kr) - \mathring{A}_m \frac{J'_m(kr_\mathrm{e})}{H'_m(kr_\mathrm{e})} H_m(kr). \tag{12}$$

In this case, not only the propagated components but also the scattered components are simultaneously synthesized due to the cylindrical baffle. Using (3) and (12), the radius-independent scattered component $\mathring{C}_m$ produced by $\mathring{D}_m(r_\mathrm{i})$ is then obtained as:

$$\mathring{C}_m = -\mathring{A}_m \frac{J'_m(kr_\mathrm{e})}{H'_m(kr_\mathrm{e})}. \tag{13}$$

Because (5) does not include the scattered components $\mathring{C}_m$, these components are undesired. To cancel out the undesired components $\mathring{C}_m$, the driving function for the exterior HOA is derived to synthesize the exterior component $\mathring{B}_m$ and also to cancel out the undesired scattered components $\mathring{C}_m$ produced by the interior HOA with $\mathring{D}_m(r_\mathrm{i})$. Similar to (11), using (7) and (9), the sound pressure produced by the exterior HOA with $\mathring{D}_m(r_\mathrm{e})$ is given by:

$$\mathring{S}_m(r_>, r_\mathrm{e}) = \frac{j\pi}{2} \mathring{D}_m(r_\mathrm{e}) \Gamma_m(r_\mathrm{e}, r_\mathrm{e}) H_m(kr) \tag{14}$$

$$= (\mathring{B}_m - \mathring{C}_m) H_m(kr). \tag{15}$$

From (14) and (15), $\mathring{D}_m(r_\mathrm{e})$ is then analytically derived as[2]:

$$\mathring{D}_m(r_\mathrm{e}) = \frac{2(\mathring{B}_m - \mathring{C}_m)}{j\pi \Gamma_m(r_\mathrm{e}, r_\mathrm{e})}$$
$$= -kr_\mathrm{e}(\mathring{B}_m H'_m(kr_\mathrm{e}) + \mathring{A}_m J'_m(kr_\mathrm{e})). \tag{16}$$

[2]The Wronskian relation $J_m(kr)H'_m(kr) - J'_m(kr)H_m(kr) = 2j/kr$ is introduced here [24, 27].

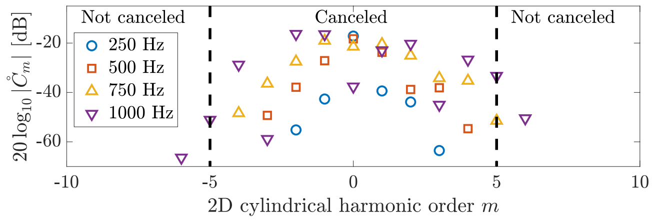

Figure 2: Scattered components $20\log_{10}|\mathring{C}_m|$ averaged over $0 \le \Phi \le \pi$.

Finally, the two continuous circular sources are discretized into two circular loudspeaker arrays (Fig. 1). When the numbers of loudspeakers for the interior and exterior arrays are L_i and L_e, the order m in (6) and (16) can be calculated up to $M_\mathrm{i} = \lfloor (L_\mathrm{i} - 1)/2 \rfloor$ and $M_\mathrm{e} = \lfloor (L_\mathrm{e} - 1)/2 \rfloor$, where $\lfloor \cdot \rfloor$ represents the floor function. For actual implementation, $L_\mathrm{i} > L_\mathrm{e}$ because $r_\mathrm{i} \gg r_\mathrm{e}$. Therefore, the scattered components $\mathring{C}_m$ for $M_\mathrm{e} < |m| \le M_\mathrm{i}$ cannot be canceled. However, most of the scattered spectra are included in the lower order components and can be sufficiently canceled using only the $|m| \le M_\mathrm{e}$ components, as shown in Fig. 2.

When $L_\mathrm{e} = 0$ and no exterior sound field is considered in (5) and (16), (5) and (6) then correspond to the decomposed global interior sound field and driving function for the conventional method with the single circular array. Therefore, the proposed method is a generalized formulation that includes the conventional method.

3. COMPUTER SIMULATIONS

The proposed method using two circular arrays was compared with the conventional method using a single circular array [13, 16] through computer simulations. A 2D free-field was assumed and the speed of sound c was 343.36 m/s. The target frequency f was in the 100 to 1,000 Hz range and the wavenumber was $k = 2\pi f/c$. The total number of loudspeakers used for both methods was 64. The numbers of loudspeakers and the radii of the circular arrays for the interior and exterior HOA in the proposed method were $L_\mathrm{i} = 53$ and $L_\mathrm{e} = 11$, and $r_\mathrm{i} = 2.0$ m and $r_\mathrm{e} = 0.2$ m, respectively. Two local sound zones with radius $R_\mathrm{l} = 0.5$ m centered at $\boldsymbol{r}_1 = [1.0, 0]$ for a bright zone and $\boldsymbol{r}_2 = [1.0, \pi]$ for a dark zone were assumed and $M = \lceil ekR_\mathrm{l}/2 \rceil$ in (5). The desired sound field in the bright zone was a simple plane wave with a direction of $0 \le \Phi \le \pi$ and $\mathring{A}_m^{(1)} = j^m e^{-jm\Phi}$. The radius of the global sound field was then set to $R = 1.5$ m. The maximum order M_i in (5) and (6) was $M_\mathrm{i} = \lceil ekR/2 \rceil$. In the conventional method with $L_\mathrm{i} = 64$ loudspeakers, if $M_\mathrm{i} > \lfloor (L_\mathrm{i} - 1)/2 \rfloor = 31$, then it was truncated to 31. In the proposed method, if $M_\mathrm{i} > \lfloor (L_\mathrm{i} - 1)/2 \rfloor = 26$, then it was truncated to 26. The maximum order M_e in (5) and (16) was $M_\mathrm{e} = \lceil ekr_\mathrm{e}/2 \rceil$. From the results of preliminary investigations, if $M_\mathrm{e} > 3$, then M_e in (5) was truncated to 3 for greater control accuracy. If the maximum order of (16) for $\mathring{C}_m$ was higher than $\lfloor (L_\mathrm{e} - 1)/2 \rfloor = 5$, it was then truncated to 5. The positive Lagrange multipliers λ_1 and λ_2 in (5) were set at 0.2 and 0.001, respectively, for both methods as in [17]. In the proposed method, the truncation order used to calculate (8) and (9) was set at 50.

To estimate the control accuracy, the synthesis error in the bright zone $\mathbb{D}_\mathrm{b}$ of $\varepsilon(\boldsymbol{r}) = 10\log_{10}(|S_\mathrm{des}(\boldsymbol{r}) - S_\mathrm{syn}(\boldsymbol{r})|^2/|S_\mathrm{des}(\boldsymbol{r})|^2)$, and the acoustic contrast between the bright zone $\mathbb{D}_\mathrm{b}$ and the dark zone $\mathbb{D}_\mathrm{d}$ of

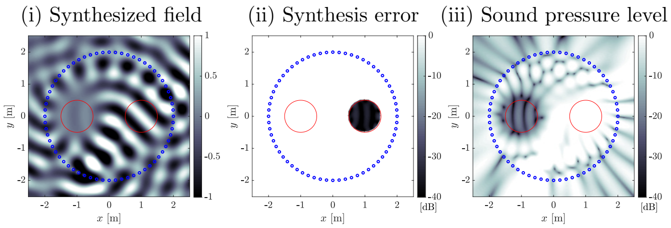

(a) Conventional method ($L_\mathrm{i} = 64, L_\mathrm{e} = 0$) : $\Phi = \pi/4$

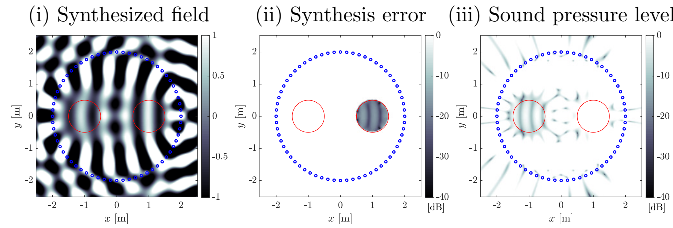

(c) Conventional method ($L_\mathrm{i} = 64, L_\mathrm{e} = 0$) : $\Phi = \pi$

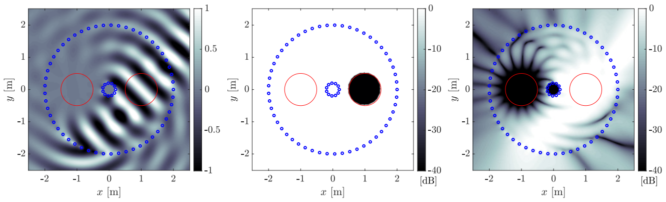

(b) Proposed method ($L_\mathrm{i} = 53, L_\mathrm{e} = 11$) : $\Phi = \pi/4$

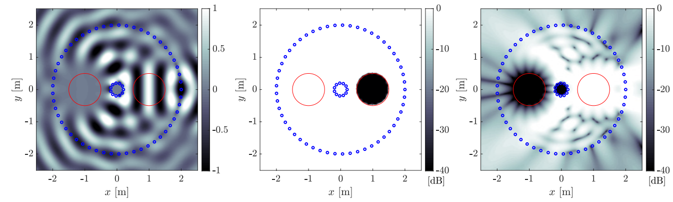

(d) Proposed method ($L_\mathrm{i} = 53, L_\mathrm{e} = 11$) : $\Phi = \pi$

Figure 3: Results for (i) synthesized sound field $S(\boldsymbol{r})$, (ii) synthesis error $\varepsilon(\boldsymbol{r})$, and (iii) sound pressure level $20\log_{10}|S(\boldsymbol{r})|$ ($\boldsymbol{r}_1 = [1.0, 0]$ was set at 0 dB) with frequency $f = 500$ Hz and plane wave directions of $\Phi = \pi/4$ and π. Blue circles represent loudspeakers.

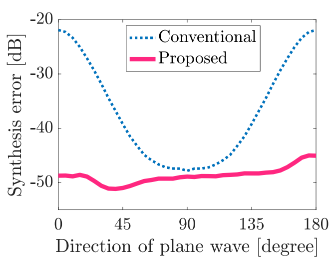

(a) Averaged for $0 \leq f \leq 1,000$

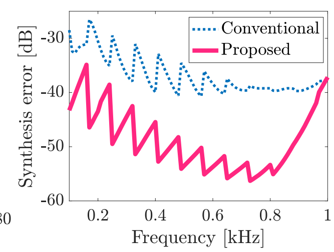

(b) Averaged for $0 \leq \Phi \leq \pi$

Figure 4: Synthesis error in bright zone.

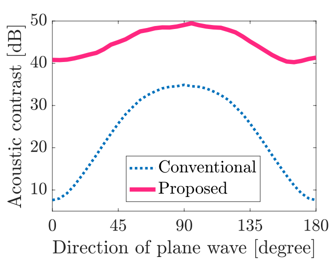

(a) Averaged for $0 \leq f \leq 1,000$

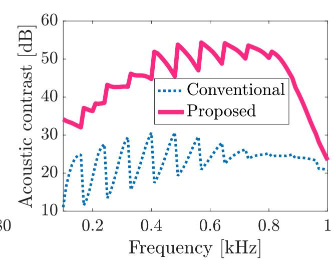

(b) Averaged for $0 \leq \Phi \leq \pi$

Figure 5: Acoustic contrast χ.

$\chi = 10\log_{10}(\int_{\mathbb{D}_\mathrm{b}}|S_\mathrm{syn}(\boldsymbol{r})|^2 d\boldsymbol{r}/\int_{\mathbb{D}_\mathrm{d}}|S_\mathrm{syn}(\boldsymbol{r})|^2 d\boldsymbol{r})$ were introduced, where $S_\mathrm{des}(\boldsymbol{r})$ and $S_\mathrm{syn}(\boldsymbol{r})$ were the desired and synthesized sound fields, respectively.

The results for the scattered components $20\log_{10}|\mathring{C}_m|$ in (13) averaged over $0 \leq \Phi \leq \pi$ are plotted in Fig. 2. These results indicate that most of the scattered spectra up to 1000 Hz can be sufficiently canceled using the proposed method, even if the maximum order in (16) ranged up to 5. The results for the synthesized sound field, the synthesis error, and the synthesized sound pressure level for both methods with $f = 500$ Hz and $\Phi = \pi/4$ and π are shown in Fig. 3. Additionally, the results for the synthesis error in

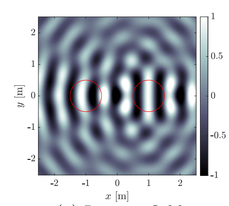

(a) Interior field

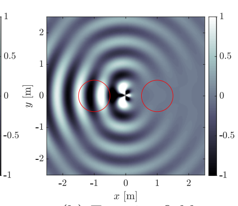

(b) Exterior field

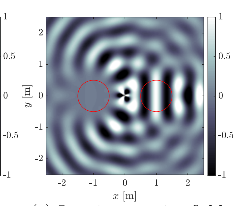

(c) Interior-exterior field

Figure 6: Reconstructed sound fields for proposed method calculated using (5), (1), (2), and (3) with $f = 500$ Hz and $\Phi = \pi$.

the bright zone $(1/\pi R_\mathrm{i}^2)\int_{\mathbb{D}_\mathrm{b}}\varepsilon(\boldsymbol{r})d\boldsymbol{r}$ and the acoustic contrast χ averaged for $100 \leq f \leq 1,000$ and $0 \leq \Phi \leq \pi$ are plotted in Figs. 4 and 5, respectively. These results show that the proposed method can avoid the occlusion problem and significantly improve both the synthesis accuracy and the acoustic contrast compared with the conventional method, which included the occlusion problem, as shown in Figs. 3(c), 4(a) and 5(a). To illustrate the physical impact of the proposed method, the reconstructed interior, exterior, and interior-exterior mixed sound fields with $f = 500$ Hz and $\Phi = \pi$ are shown in Fig. 6. The sound pressures propagating into the dark zone via the interior field (Fig. 6(a)) can be successfully canceled using the pressures with the opposite phase from the exterior field (Fig. 6(b)) in the total mixed field (Fig. 6(c)). Consequently, the proposed method can avoid the occlusion problem and provide improved control accuracy by introducing interior-exterior sound field separation and synthesis.

4. CONCLUSIONS

This paper proposed a 2D multizone sound field synthesis method using two circular arrays with a cylindrical baffle. The global sound field is defined as a mixture of the interior and exterior sound fields based on sound field separation. The separated global interior and exterior sound fields are then simultaneously synthesized via interior-exterior HOA. Computer simulations validated the effectiveness of the proposed method using two circular arrays.

5. REFERENCES

[1] J. Ahrens and S. Spors, “An analytical approach to sound field reproduction using circular and spherical loudspeaker distributions,” *Acta Acust. Acust.*, vol. 94, no. 6, pp. 988–999, Nov. 2008.

[2] Y. J. Wu and T. D. Abhayapala, “Theory and design of soundfield reproduction using continuous loudspeaker concept,” *IEEE Trans. Speech, Audio, Lang. Process.*, vol. 17, no. 1, pp. 107–116, Jan. 2009.

[3] J.-W. Choi and Y.-H. Kim, “Generation of an acoustically bright zone with an illuminated region using multiple sources,” *J. Acoust. Soc. Am.*, vol. 111, no. 4, pp. 1695–1700, Apr. 2002.

[4] T. Okamoto and A. Sakaguchi, “Experimental validation of spatial Fourier transform-based multiple sound zone generation with a linear loudspeaker array,” *J. Acoust. Soc. Am.*, vol. 141, no. 3, pp. 1769–1780, Mar. 2017.

[5] T. Betlehem, W. Zhang, M. Poletti, and T. Abhayapala, “Personal sound zones: Delivering interface-free audio to multiple listeners,” *IEEE Signal Process. Mag.*, vol. 32, no. 2, pp. 81–91, Mar. 2015.

[6] M. Poletti, “An investigation of 2D multizone surround sound systems,” in *Proc. 125th Conv. Audio Eng. Soc.*, Oct. 2008.

[7] T. Betlehem and P. D. Teal, “A constrained optimization approach for multi-zone surround sound,” in *Proc. ICASSP*, May 2011, pp. 437–440.

[8] N. Radmanesh and I. S. Burnett, “Generation of isolated wideband sound fields using a combined two-stage Lasso-LS algorithm,” *IEEE Trans. Audio, Speech, Lang. Process.*, vol. 21, no. 2, pp. 378–387, Feb. 2013.

[9] W. Jin and W. B. Kleijn, “Theory and design of multizone soundfield reproduction using sparse methods,” *IEEE/ACM Trans. Audio, Speech, Lang. Process.*, vol. 23, no. 12, pp. 2343–2355, Dec. 2015.

[10] N. Radmanesh, I. S. Burnett, and B. D. Rao, “A Lasso-LS optimization with a frequency variable dictionary in a multizone sound system,” *IEEE/ACM Trans. Audio, Speech, Lang. Process.*, vol. 24, no. 3, pp. 583–593, Mar. 2016.

[11] M. Buerger, C. Hofmann, and W. Kellermann, “Broadband multizone sound rendering by jointly optimizing the sound pressure and particle velocity,” *J. Acoust. Soc. Am.*, vol. 143, no. 3, pp. 1477–1490, Mar. 2018.

[12] J. Donley, C. H. Ritz, and W. B. Kleijn, “Multizone soundfield reproduction with privacy and quality based speech masking filters,” *IEEE/ACM Trans. Audio, Speech, Lang. Process.*, vol. 26, no. 6, pp. 1041–1055, June 2018.

[13] Y. J. Wu and T. D. Abhayapala, “Spatial multizone soundfield reproduction: Theory and design,” *IEEE Trans. Audio, Speech, Lang. Process.*, vol. 19, no. 6, pp. 1711–1720, Aug. 2011.

[14] M. A. Poletti and F. M. Fazi, “An approach to generating two zones of silence with application to personal sound systems,” *J. Acoust. Soc. Am.*, vol. 137, no. 2, pp. 598–605, Feb. 2015.

[15] ——, “Generation of half-space sound fields with application to personal sound systems,” *J. Acoust. Soc. Am.*, vol. 139, no. 3, pp. 1294–1302, Mar. 2016.

[16] W. Zhang, T. D. Abhayapala, T. Betlehem, and F. M. Fazi, “Analysis and control of multi-zone sound field reproduction using modal-domain approach,” *J. Acoust. Soc. Am.*, vol. 140, no. 3, pp. 2134–2144, Sept. 2016.

[17] W. Zhang, J. Zhang, T. D. Abhayapala, and L. Zhang, “2.5D multizone reproduction using weighted mode matching,” in *Proc. ICASSP*, Apr. 2018, pp. 476–480.

[18] Z. Han, M. Wu, Q. Zhu, and J. Yang, “Two-dimensional multizone sound field reproduction using a wave-domain method,” *J. Acoust. Soc. Am.*, vol. 144, no. 3, pp. EL185–EL190, Sept. 2018.

[19] N. Ueno, S. Koyama, and H. Saruwatari, “Three-dimensional sound field reproduction based on weighted mode-matching method,” *IEEE/ACM Trans. Audio, Speech, Lang. Process.*, vol. 27, no. 12, pp. 1852–1867, Dec. 2019.

[20] Q. Zhu, X. Qiu, P. Coleman, and I. Burnett, “A comparison between two modal domain methods for personal audio reproduction,” *J. Acoust. Soc. Am.*, vol. 147, no. 1, pp. 161–173, Jan. 2020.

[21] J. Zhang, W. Zhang, T. D. Abhayapala, and L. Zhang, “2.5D multizone reproduction using weighted mode matching: Performance analysis and experimental validation,” *J. Acoust. Soc. Am.*, vol. 147, no. 3, pp. 1404–1417, Mar. 2020.

[22] A. Fahim, P. Samarasinghe, and T. D. Abhayapala, “Extraction of exterior field from a mixed sound field for 2D height-invariant sound propagation,” in *Proc. IWAENC*, Sept. 2016.

[23] ——, “Sound field separation in a mixed acoustic environment using a sparse array of higher order spherical microphones,” in *Proc. HSCMA*, Mar. 2017, pp. 151–155.

[24] M. A. Poletti and T. D. Abhayapala, “Interior and exterior sound field control using general two-dimensional first-order sources,” *J. Acoust. Soc. Am.*, vol. 129, no. 1, pp. 234–244, Jan. 2011.

[25] T. Okamoto, “Analytical approach to 2.5D sound field control using a circular double-layer array of fixed-directivity loudspeakers,” in *Proc. ICASSP*, Mar. 2017, pp. 91–95.

[26] ——, “Mode-matching-based sound field recording and synthesis with circular double-layer arrays,” *Appl. Sci.*, vol. 8, no. 7, 1048, July 2018.

[27] E. G. Williams, *Fourier Acoustics: Sound Radiation and Nearfield Acoustic Holography*. London: Academic Press, 1999.

[28] P. Samarasinghe, T. Abhayapala, and M. Poletti, “Wavefield analysis over large areas using distributed higher order microphones,” *IEEE/ACM Trans. Audio, Speech, Lang. Process.*, vol. 22, no. 3, pp. 647–658, Mar. 2014.

[29] R. A. Kennedy, P. Sadeghi, T. D. Abhayapala, and H. M. Jones, “Intrinsic limits of dimensionality and richness in random multipath fields,” *IEEE Trans. Signal Process.*, vol. 55, no. 6, pp. 2542–2556, June 2007.

[30] P. A. Martin, *Multiple Scattering: Interaction of Time-Harmonic Waves with N Obstacles*. New York: Cambridge University press, 2006.

[31] T. Okamoto, “Analytical methods of generating multiple sound zones for open and baffled circular loudspeaker arrays,” in *Proc. WASPAA*, Oct. 2015.